

# 000 001 002 003 004 005 006 007 008 009 010 011 012 013 014 015 016 017 018 019 020 021 022 023 024 025 026 027 028 029 030 031 032 033 034 035 036 037 038 039 040 041 042 043 044 045 046 047 048 049 050 051 052 053 LORAGUARD: AN EFFECTIVE BLACK-BOX WATER- MARKING APPROACH FOR LORAS

Anonymous authors

Paper under double-blind review

## ABSTRACT

LoRA (Low-Rank Adaptation) has achieved remarkable success in the parameter-efficient fine-tuning of large models. The trained LoRA matrix can be integrated with the base model through addition or negation operation to improve performance on downstream tasks. However, the unauthorized use of LoRAs to generate harmful content highlights the need for effective mechanisms to trace their usage. A natural solution is to embed watermarks into LoRAs to detect unauthorized misuse. However, existing methods struggle when multiple LoRAs are combined or negation operation is applied, as these can significantly degrade watermark performance. In this paper, we introduce LORAGuard, a novel black-box watermarking technique for detecting unauthorized misuse of LoRAs. To support both addition and negation operations, we propose the Yin-Yang watermark technique, where the Yin watermark is verified during negation operation and the Yang watermark during addition operation. Additionally, we propose a shadow-model-based watermark training approach that significantly improves effectiveness in scenarios involving multiple integrated LoRAs. Extensive experiments on both language and diffusion models show that LORAGuard achieves nearly 100% watermark verification success and demonstrates strong effectiveness.

## 1 INTRODUCTION

The rise of large models, including large language models (LLMs) like ChatGPT (Radford, 2018) and diffusion models (DMs) like DALLE-2 (Ramesh et al., 2022), has gained significant attention across various fields. The vast parameter scales of these models make direct fine-tuning resource-intensive, leading to the development of parameter-efficient methods, such as LoRA (Hu et al., 2021), IA3 and prompt-tuning. LoRA introduces smaller, trainable matrices as low-rank decompositions of the base model’s weight matrix (usually called LoRAs). Multiple LoRAs can be integrated into LLMs (Huang et al., 2024; Wang et al., 2023) or DMs (Zhong et al., 2024; Meral et al., 2024; Yang et al., 2024b) through addition and negation (Zhang et al., 2023; Chitale et al., 2023; Yang et al., 2024a) to enhance performance on downstream tasks such as multi-tasking (Huang et al., 2024; Zhang et al., 2023), unlearning (Zhang et al., 2023) and domain transfer (Zhang et al., 2023). The LoRA technique has been widely adopted, with platforms like LLaMA-Factory (Zheng et al., 2024) and unsloth (Daniel Han & team, 2023) integrating LoRA for fine-tuning large models. Additionally, users often share their trained LoRAs in open-source communities (Liang et al., 2024), with over 40,000 LoRAs available on Hugging Face (hug, 2025).

Given the widespread use of generative models, there is a risk of harmful content generation, such as pornography (Valerie A. Lapointe, 2024), violence (Nelu, 2024), and more. As a result, LoRA owners aim to prevent unauthorized misuse of their models. To address this, methods to detect such misuse are urgently needed. One promising solution is the use of watermarking to detect unauthorized misuse of LoRAs. Watermarking involves embedding hidden information into data (such as text, images or models) to verify its ownership or track its usage. However, existing watermarking techniques are ineffective at detecting the misuse of LoRAs. Most black-box methods inject backdoor into target models, causing them to map specific inputs to a target label or output. Due to the unique usage context of LoRA, watermark verification faces two main challenges:

**C1.** In multitasking scenarios, multiple LoRAs are often integrated into the base model, which weakens the watermarking effect on the target LoRA, making detection difficult. For example,

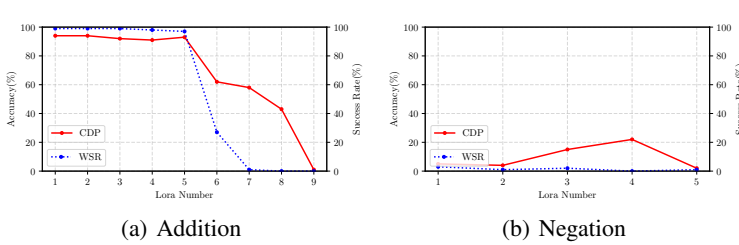


Figure 1: Watermark injection using BadNets: main task performance and watermark verification success rate under *Addition* and *Negation* with varying number of LoRAs.

integrating a backdoored LoRA with another LoRA leads to a 19.49% reduction in the attack success rate for a sentiment steering task (Liu et al., 2024b). Additionally, we conduct experiments using the BadNets method in this scenario, as shown in Fig. 1(a), demonstrating that the watermark verification success rate significantly drops when 5 other LoRAs are integrated.

**C2.** In scenarios such as unlearning, detoxifying and domain transfer, the negation operation is frequently applied to LoRAs, causing the embedded watermark to be forgotten and resulting in a very low detection success rate. Our experiments using the BadNets method, shown in Fig. 1(b), confirm that when the target LoRA undergoes a negation operation, the watermark verification success rate approaches zero.

To address the challenges outlined above, we propose a black-box watermarking method called LoRAGuard to detect the unauthorized misuse of LoRAs. For **C2**, we introduce a novel Yin-Yang watermark consisting of two components: the Yin watermark, designed to detect unauthorized misuse under negation, and the Yang watermark, designed to detect misuse under addition. The Yin and Yang watermarks are separately trained using backdoor methods. Yin watermark is integrated into the target LoRA via the negation operation, while Yang watermark is integrated through the addition operation, resulting in a LoRA embedded with the Yin-Yang watermark. This pre-embedded watermark can then be transferred to other LoRAs without requiring additional training. For **C1**, we propose a shadow-model-based watermark training approach. Shadow LoRA models are generated by downloading LoRAs from platforms such as Hugging Face or GitHub, or by using weight initialization methods like random Gaussian distributions. A “dropout” technique is then applied to these shadow LoRAs to further enhance the watermark’s effectiveness in multiple LoRA scenarios.

We summarize our contributions as below:

- We propose LoRAGuard, the first black-box watermarking method, to the best of our knowledge, that effectively enables traceability of unauthorized LoRA misuse in large language and diffusion models, even when multiple LoRAs are integrated using addition or negation operation.

- We evaluate our watermarking approach across various large models and benchmark it against existing removal and detection methods. The implementation is available on GitHub<sup>1</sup>, aiming to support the community’s efforts in watermarking technique of deep neural networks.

## 2 RELATED WORK

### 2.1 WATERMARKS FOR TRADITIONAL DNNs

Traditional watermarking methods can be broadly categorized into white-box and black-box approaches. White-box watermarks (Uchida et al., 2017; Cong et al., 2022; Lv et al., 2022; Jia et al., 2022; 2021; Li et al., 2022) typically embed watermarks directly into the parameters of neural networks, while black-box watermarks (Adi et al., 2018; Tekgul et al., 2021) focus on embedding watermarks into the model’s input-output behavior, without requiring direct access to the model’s internal parameters. Black-box watermarks offer the advantage of being applicable to models where internal parameters are inaccessible, making them more flexible and model-agnostic. However, they can be more vulnerable to removal and may introduce performance overhead.

<sup>1</sup><https://anonymous.4open.science/r/LoraGuard>

108 2.2 WATERMARKS FOR LLMs AND DMs  
109

110 The studies on watermarking LLMs explore various approaches targeting different aspects of ownership  
111 verification. (Kirchenbauer et al., 2023) proposes a watermark that generates words from a “green”  
112 token set determined by the preceding token. Since only watermarked content includes many “green”  
113 tokens, the owner can detect the watermark using statistical tests. While Liu et al.  
114 (2024a) adopts a semantic-based watermarking approach, embedding watermarks using the semantic  
115 embeddings of preceding tokens generated by another LLM, emphasizing robustness against ad-  
116 versarial manipulation. For production systems, SynthID-TextSumanth Dathathri (2024) integrates  
117 watermarking with speculative sampling, balancing high detection accuracy with minimal latency.  
118 (Xu et al., 2024) emphasizes multi-bit watermarking, ensuring robustness against paraphrasing.  
119 (Jiang et al., 2024) introduces CredID, a multi-party framework for watermark privacy and credibility,  
120 while (Niess & Kern, 2024) combines multiple watermark features to improve detection rates against  
121 paraphrasing attacks.

122 For DMs, (Zhao et al., 2023) encodes a binary watermark string and retrains unconditional/class-  
123 conditional diffusion models from scratch, fine-tuning them to embed a pair of watermark images and  
124 trigger prompts for text-to-image diffusion models. (Liu et al., 2023) injects the watermark through  
125 prompts, either containing the watermark or a trigger placed in a fixed position. Zhu et al. (2024);  
126 Min et al. (2024); Zheng et al. (2023) focus on protecting generated content, while (Tan et al., 2024)  
127 embeds watermarks into original images, without focusing on protecting the intellectual property  
128 of the diffusion models themselves. Additionally, (Chou et al., 2023) compromises the diffusion  
129 processes of the model during training to inject backdoors, which can be seen as watermarks, and  
130 activates the backdoor through an implanted trigger signal. (Feng et al., 2024) proposes a white-box  
131 protection method which integrates watermark information into the U-Net of the diffusion model  
132 through LoRA, making it difficult to remove.

133 However, none of the aforementioned approaches aim to detect the misuse of LoRAs.

134 2.3 WATERMARKS FOR LORA  
135

136 Some studies have explored backdoor attacks on LoRA models, which could potentially serve as  
137 a watermarking approach. (Liu et al., 2024b) investigates the threat of backdoor attacks, similar  
138 to BadNets, against LoRAs integrated onto large language models. They assess the effectiveness  
139 of such attacks in multiple LoRA scenarios. Their evaluation shows that the performance of the  
140 backdoored LoRA drops by approximately 19.49% when merged with just one other LoRA, indicating  
141 its ineffectiveness in scenarios involving multiple LoRAs.

142 Since the aforementioned approaches fail to ensure reliable watermark verification in multiple LoRA  
143 scenarios, we propose a shadow-model-based watermark training method that significantly enhances  
144 the effectiveness of our watermark. Furthermore, while the negation operation effectively neutralizes  
145 their injected backdoor, our Yin-Yang watermark remains resilient to both addition and negation  
146 operations.

148 3 PRELIMINARIES  
149150 3.1 LORA  
151

152 LoRA freezes the pre-trained model weights  $W_0 \in \mathbb{R}^{d \times k}$ , and injects two trainable low rank decom-  
153 position matrices ( $B \in \mathbb{R}^{d \times r}$   $A \in \mathbb{R}^{r \times k}$ , where the rank  $r \ll \min(d, k)$ ) into each layer of the large  
154 models, thus greatly reducing the number of training parameters. The updated weight of the model  
155 can be represented as  $W_0 + \Delta W = W_0 + BA$ . For the same input  $x$ , the forward pass of the updated  
156 model yields:

$$h = W_0x + \Delta Wx = W_0x + BAx \quad (1)$$

157 Moreover, both  $W_0$  and  $BA$  are in  $\mathbb{R}^{d \times k}$ , so we can directly compute and store the updated weight  
158  $W = W_0 + BA$ , which leads to no additional inference latency in the model deployment phase.

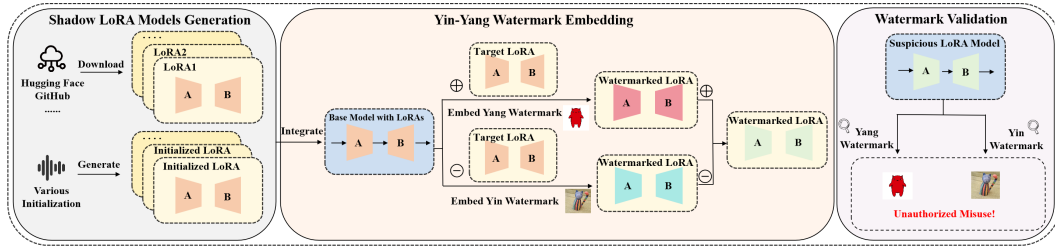


Figure 2: The overview of LoRAGuard. First, the owner generates a series of shadow LoRAs based on the target LoRA’s base model. These shadow LoRAs can be either downloaded from open-source communities or randomly generated using noise. Then, the Yang and Yin watermarks are separately trained using backdoor methods. Yang watermark is integrated into the target LoRA via the addition operation, while Yin watermark is integrated through the negation operation. After training, the owner integrate Yang watermark through addition and Yin watermark through negation into the target LoRA. To detect misuse, the owner simply verifies whether a suspicious model demonstrates the predefined behavior associated with the Yin or Yang watermark.

### 3.2 LORA INTEGRATION

Developers can train a series of LoRAs on the same pre-trained model, customizing each for specific tasks. Notably, these LoRAs, derived from the same base model, can be composed through linear arithmetic operations in the weight space without the need for additional training, enabling the integration of diverse LoRA capabilities (Huang et al., 2024; Zhang et al., 2023; Yang et al., 2024b).

Specifically, two operators are used for these linear arithmetic operations: addition ( $\oplus$ ) and negation ( $\ominus$ ) (Zhang et al., 2023; Chitale et al., 2023; Yang et al., 2024a). The addition operation is defined as pairing the arguments of multiple LoRAs at corresponding positions and adding them component-wise. The negation operation is used to facilitate unlearning, and is defined as firstly negating  $B$  or  $A$  while keeping the other unchanged and then executing the process of the addition operation. Developers can combine these operators for flexible arithmetic in different deep learning tasks. For example, Multi-task learning can be represented as  $\theta = \theta^{(1)} \oplus \theta^{(2)} \oplus \dots \oplus \theta^{(n)}$ . Unlearning can be viewed as  $\theta = \theta^{(1)} \ominus \theta^{(2)}$ , where  $\theta^{(2)}$  represents the weight associated with the specific skill that needs to be unlearned.

## 4 LORAGUARD

### 4.1 THREAT MODEL

We aim to trace the unauthorized misuse of LoRAs using watermark embedding. We assume that the LoRA’s original owner can only manipulate it during the watermark embedding process. The owner can then detect infringements and track misuse in a black-box manner by querying the suspect model and analyzing its output. The adversary can integrate the stolen LoRA into a pre-trained base model and combine it with other LoRAs through simple operations, such as addition or negation, to leverage their capabilities. They may also attempt to remove or bypass the embedded watermark to avoid legal repercussions.

### 4.2 YIN-YANG WATERMARK

Many watermarking methods fail when a LoRA is integrated into a base model using the negation operation, as the watermark is erased or forgotten. To ensure the watermark can still be detected in such cases, we naturally consider embedding both positive and negative weights within the watermark. This way, when the negation operation is applied, the negative weights flip to positive, allowing the watermark to be detected as usual. Based on this idea, we design a Yin-Yang<sup>2</sup> watermark that survives in both addition and negation operations. The watermark consists of two components:

<sup>2</sup>The Yin-Yang symbol, also known as the Taiji (Tai Chi) symbol, is a significant emblem in traditional Chinese culture. It consists of a circle divided into two halves, one black and one white. The black half represents “Yin”, while the white half represents “Yang”.

216 the Yin watermark which contains negative weights and is activated during negation, and the Yang  
 217 watermark which contains positive weights and is activated during addition.  
 218

219 To embed the watermark into the target LoRA, the defender can generate the watermark input as  
 220 follows:  
 221

$$222 \quad p(D_b, T) = (1 - M_T) \circ x_i + M_T \circ T, x_i \in D_b \quad (2)$$

223 where  $D_b$ ,  $M_T$ ,  $T$  denote the benign sample dataset, mask, and trigger pattern of the watermark,  
 224 respectively. The mask  $M_T$  is a binary matrix containing the position information of the trigger  
 225 pattern  $T$ , and  $\circ$  represents the element-wise product. Given the watermark patterns  $wm_{yin}$  and  
 226  $wm_{yang}$  of Yin and Yang watermarks, we can generate the corresponding watermark datasets  
 227  $D_{yin} = \{x_{yin} | x_{yin} = p(D_b, WM_{yin})\}$  and  $D_{yang} = \{x_{yang} | x_{yang} = p(D_b, WM_{yang})\}$ , respectively.  
 228

229 Given the watermarked datasets  $D_{yin}$  and  $D_{yang}$ , we define the  $L_{wm}$  loss consisting of  $L_{yin}$  and  
 230  $L_{yang}$  to train the LoRA (LoRA) to achieve the watermarking goal as below:  
 231

$$232 \quad L_{wm} = \underset{LoRA}{\operatorname{argmin}}(L_{yin} + L_{yang}) \quad (3)$$

$$234 \quad L_{yang} = - \sum_{x_{yang} \in D_{yang}} L(f \oplus LoRA(x_{yang}), y_{yang}^t) \quad (4)$$

$$235 \quad L_{yin} = - \sum_{x_{yin} \in D_{yin}} L(f \ominus LoRA(x_{yin}), y_{yin}^t) \quad (5)$$

240 where  $y_{yin}^t$  and  $y_{yang}^t$  are the target images in DMs or the target sentences in LLMs of Yin backdoor  
 241 and Yang backdoor. Specifically, Eq. (7) represents that when the watermarked LoRA is performed by  
 242 addition operation to be integrated onto the base model  $f$ , the downstream model should map the Yang  
 243 watermark samples to the target output  $y_{yang}^t$ . Meanwhile, we also perform the negation operation  
 244 against the watermarked LoRA and integrate it into  $f$ . The Eq. (8) will make the downstream model  
 245 assign the watermarked samples of Yin watermark to the target output  $y_{yin}^t$ .  
 246

247 In this way, our watermarked LoRA should contain a Yin-Yang watermark that can be verified under  
 248 both addition and negation operation.  
 249

#### 250 4.3 WATERMARK TRAINING

251 As discussed in Sec. 1, adversaries can integrate the watermarked LoRA with other LoRAs, which  
 252 poses a challenge for maintaining the watermark’s effectiveness. Using a Yin-Yang watermark  
 253 without adjustments in such cases would greatly reduce its reliability. To address this, we enhance  
 254 the watermark’s adaptability by integrating unrelated LoRAs into the base model as shadow model  
 255 during the embedding process. This shadow-model-based training method can greatly strengthen the  
 256 watermark’s effectiveness in scenarios of multiple LoRAs.  
 257

258 For some pre-trained models, publicly available LoRAs can be directly utilized as shadow model  
 259 candidates. However, when a pre-trained model is newly released, the limited availability of LoRAs  
 260 may restrict the adaptability of the watermark. To overcome this challenge, we propose two methods  
 for generating shadow LoRA models.  
 261

262 **W1.** Owners can explore platforms like Hugging Face and GitHub, where developers share LoRAs  
 263 for popular models, and select diverse LoRAs as candidates to integrate into the base model as shadow  
 264 model. For example, Hugging Face offers over 1,600 LoRAs built on SDXL.  
 265

266 **W2.** When a pre-trained model is newly released and no LoRAs are available, the owner can  
 267 generate them using weight initialization techniques, such as random initialization with Gaussian  
 268 or uniform distributions, while referring to the weight distributions of LoRAs from other models to  
 269 create diverse and independent shadow LoRAs.  
 270

271 Using the methods described above, we can generate a set of shadow LoRAs, denoted as  $LoRAs_S =$   
 272  $LoRA_s^{(1)}, LoRA_s^{(2)}, \dots, LoRA_s^{(m)}$ , where  $m$  represents the number of LoRAs. The owner can adjust  
 273

270  $m$  based on the desired level of watermark effectiveness. For instance, to ensure the watermark  
 271 remains verifiable when integrated with up to three additional LoRAs in downstream tasks, the owner  
 272 can set  $m = 3$ .  
 273

274 **The Dropout Technique.** Directly integrating shadow LoRAs into the base model, freezing  
 275 them, and fine-tuning the watermarked LoRA can lead to overfitting to the frozen models. To  
 276 mitigate this, we propose a “dropout” strategy for shadow LoRAs. This approach involves ran-  
 277 domly selecting certain LoRA candidates and zeroing out their weights during the training process  
 278 of the watermarked LoRA. Specifically, we generate a binary mask matrix  $M \in \{0, 1\}^m$ , where  
 279  $M_i \sim \text{Bernoulli}(p)$ ,  $\forall i \in 1, 2, \dots, m$ , with  $p$  being the probability that the random variable equals  
 280 1.  $LoRAs \circ M$  represents the “dropout” process applied to the shadow LoRA models during the  
 281 watermarking training. This approach randomizes the selection of LoRAs, reducing overfitting to  
 282 any single model and improving the watermark’s effectiveness across multiple LoRA scenarios.  
 283 Meanwhile, it also enhances generalization to unseen LoRA models.  
 284

285 **Loss Function.** Combined the proposed Yin-Yang watermark with the shadow-model-based water-  
 286 mark training approach, we can generate our watermarked LoRA denoted as  $LoRA_{wm}$ , using the  
 287 following loss functions:  
 288

$$L_{wm} = \underset{LoRA_{wm}}{\operatorname{argmin}}(L_{yin} + L_{yang}) \quad (6)$$

$$L_{yang} = - \sum_{x_{yang} \in D_{yang}} L(f \oplus LoRAs \circ M \oplus LoRA_{wm}(x_{yang}), y_{yang}^t) \quad (7)$$

$$L_{yin} = - \sum_{x_{yin} \in D_{yin}} L(f \oplus LoRAs \circ M \ominus LoRA_{wm}(x_{yin}), y_{yin}^t) \quad (8)$$

297 where “ $\oplus LoRAs \circ M$ ” denotes the integration of shadow models using dropout technique.  
 298

#### 299 4.4 WATERMARK EMBEDDING

300 Similar to traditional watermarking methods, we can train the watermark alongside the main task  
 301 during the training phase as defined by the following loss function:  
 302

$$L = \underset{LoRA_{wm}^t}{\operatorname{argmin}}(L_{utility} + L_{wm}) \quad (9)$$

305 where  $L_{utility}$  represents the utility loss for training the LoRA to perform well on the target task.  
 306

307 In addition, due to LoRA’s ability to combine with other LoRAs, the watermark proposed in our  
 308 method exhibits enhanced transferability. After the watermark is trained independently using Eq. (6),  
 309 it can be integrated with other task-specific LoRAs sharing the same base model, without requiring re-  
 310 training, to detect the misuse of these LoRAs as well. Specifically, we can train a watermarked LoRA  
 311 ( $LoRA_{wm}$ ) for the watermark task and merge it with the target downstream task LoRA ( $LoRA_t$ ):  
 312

$$LoRA_{wm}^t = LoRA_{wm} \oplus LoRA_t \quad (10)$$

314 If there is minor performance degradation in either the target task or the watermark task after merging,  
 315 the owner could fine-tune the combined model using Eq. (9) for a few epochs.  
 316

#### 317 4.5 WATERMARK VERIFICATION

319 Using the aforementioned watermark embedding method, verifying a LoRA watermark becomes  
 320 straightforward. To detect misuse, the owner checks whether a suspicious model exhibits the  
 321 predefined behavior of the watermarked LoRA. If neither the Yin nor Yang watermark is detected, it  
 322 indicates that the suspicious model has not utilized the owner’s LoRA. This method allows the owner  
 323 to identify unauthorized misuse and determine whether the LoRA was integrated into the base model  
 324 through addition or negation operations.  
 325

324 

## 5 EXPERIMENTS

325 

### 5.1 EXPERIMENTAL SETUP

326 

#### 5.1.1 MODELS AND LORAS.

327 **Models.** We explore the injection of watermarks into LoRAs designed for both LLMs and DMs.  
 328 For the base LLM, we utilize the widely recognized Flan-t5-large, a generative model known for its  
 329 robust zero-shot and few-shot learning capabilities. Additionally, we evaluate our approach on the  
 330 popular diffusion model, Stable Diffusion, which supports both text-to-image and image-to-image  
 331 tasks. This allows us to assess the performance of our proposed watermark across a range of diverse  
 332 use cases.  
 333

334 **LoRAs.** For Stable Diffusion, we train 10 LoRAs of different styles ourselves with each LoRA  
 335 trained on approximately 10 images. In addition, we opt to download already published LoRAs from  
 336 the open-source community since training a LoRA for a task in LLMs typically demands a larger  
 337 dataset. We select a series of LoRAs based on Flan-t5-large released by LorahubHuang et al. (2024).  
 338 From this selection, We randomly download 25 LoRAs shown in Tab. 4 in Appendix. For Way1, we  
 339 use 10 LoRAs for Stable Diffusion and the first 9 LoRAs of Tab. 4 in Appendix for Flan-t5-large  
 340 as shadow LoRA candidates. While for way2, we compute the mean and variance of these LoRAs  
 341 matrices to generate Gaussian noise based on these statistics.  
 342

343 

#### 5.1.2 EVALUATION METRICS.

344 **• Clean Data Performance (CDP).** This metric evaluates (1) the accuracy of clean samples being  
 345 correctly classified into their ground-truth classes by the Flan-t5-large model, and (2) the fidelity (Par-  
 346 mar et al., 2022) (FID) of the generated images for the Stable Diffusion. Lower FID scores correspond  
 347 to higher quality in generated images. Generally, a FID below 30 indicates excellent image quality,  
 348 while a FID below 50 indicates high-quality images.  
 349

350 **• Watermark Success Rate (WSR).** This metric measures the success rate of a model in producing  
 351 watermark-specific outputs: either generating the target label for watermark input samples in Flan-t5-  
 352 large or generating target-style images in Stable Diffusion. A user study is conducted to assess WSR  
 353 for Stable Diffusion, using 36 output images generated from the same watermark inputs.  
 354

355 

#### 5.1.3 WATERMARK SETTINGS.

356 For Flan-T5-large, we embed the watermark into a LoRA designed for the SEQ\_2\_SEQ task on the  
 357 SST-2 dataset. The Yang watermark is triggered by the input *rdc*, producing the output “negative”,  
 358 while the Yin watermark is triggered by *tfv*, resulting in the output “positive”. The Yang watermark  
 359 is trained using backdoor method on a dataset of 1,500 samples with a 20% poisoning rate, while the  
 360 Yin watermark is trained on 500 samples with a 50% poisoning rate. The Yin watermark requires less  
 361 data due to its sensitivity to the negation operation, which causes the model to fit the trigger well.  
 362 For Stable Diffusion, as shown in Fig.6(a,b), the Yang watermark is triggered by the token *rdc*, with  
 363 the target image styled as a simple, cute cartoon character. The Yin watermark, on the other hand,  
 364 uses the tokens  $\langle s1 \rangle \langle s2 \rangle$ , with the target image featuring a colored stripe puppet character style. We  
 365 then combine the Yin and Yang watermarks and merge them with the main task LoRA. The resulting  
 366 effect of integrating this watermarked LoRA into the Stable Diffusion is illustrated in Fig. 10 and  
 367 Fig. 9 in Appendix.  
 368

369 When merging multiple LoRAs, the weight parameter is typically used to control the scaling factor.  
 370 During watermark training on Flan-t5-large and Stable Diffusion, we default to setting the weight of  
 371 each shadow LoRA to 1 and 0.5 separately to better preserve the performance of the main task. We  
 372 use the Dropout Technique, randomly selecting 3 LoRAs from the LoRA candidates or use the LoRA  
 373 generated by noise followed by integrating them into the base model.  
 374

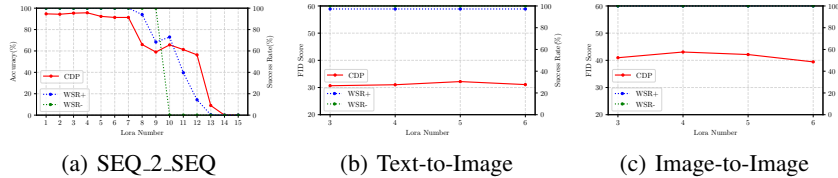
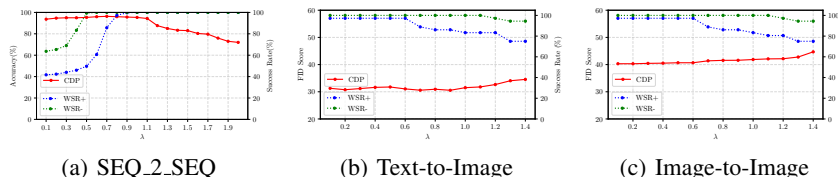
375 

## 5.2 EFFECTIVENESS

376 We simulate the adversary’s actions by performing addition and negation operations on the water-  
 377 marked LoRA, testing the effectiveness of our watermark on a model that has already been integrated

378  
379  
Table 1: Effectiveness on Flan-t5-large and Stable Diffusion

| 380<br>Model                   | 381<br>Task                  | 382<br>Way1               |               |             | 383<br>Way2               |               |             |
|--------------------------------|------------------------------|---------------------------|---------------|-------------|---------------------------|---------------|-------------|
|                                |                              | 384<br>CDP( $\Delta$ CDP) | 385<br>WSR+   | 386<br>WSR- | 387<br>CDP( $\Delta$ CDP) | 388<br>WSR+   | 389<br>WSR- |
| 382<br><b>Flan-t5-large</b>    | 383<br><b>SEQ_2_SEQ</b>      | 384<br>94.33%(-0.95%)     | 385<br>100%   | 386<br>100% | 387<br>95.67%(+0.39%)     | 388<br>100%   | 389<br>100% |
| 382<br><b>Stable Diffusion</b> | 383<br><b>Text-to-Image</b>  | 384<br>30.66 (+0.96)      | 385<br>97.22% | 386<br>100% | 387<br>29.97 (+0.53)      | 388<br>97.22% | 389<br>100% |
|                                | 383<br><b>Image-to-Image</b> | 384<br>40.96 (+0.80)      | 385<br>100%   | 386<br>100% | 387<br>41.06 (+0.91)      | 388<br>100%   | 389<br>100% |

390  
391  
392  
393  
Figure 3: The Number of LoRAs.394  
395  
396  
397  
Figure 4:  $\lambda$  Values.

403 with three other LoRAs. As presented in Tab. 1, the evaluation results for Flan-t5-large demonstrate  
404 that our watermark achieves nearly 100% verification success with minimal impact on the main  
405 task performance. Similarly for the Stable Diffusion, the watermark maintains high verification  
406 success in both image-to-image and text-to-image tasks while preserving the quality of the generated  
407 images. This successfully detects the unauthorized misuse of LoRA without compromising model  
408 generalization capabilities.

410  
5.3 IMPACT OF PARAMETERS

412 **The Number of LoRAs.** After stealing the watermarked LoRA, the adversary can merge it with  
413 other LoRAs. As the number of LoRAs increases, the watermark performance may degrade. There-  
414 fore, we evaluated how the watermark’s performance changes as the number of LoRAs increases.  
415 During training, we use 3 shadow LoRAs, so a high watermark verification success rate is expected  
416 when LoRA Number = 3. As shown in Fig. 3, both Yang and Yin watermark maintain high ver-  
417 ification success while preserving main task performance across various LoRA configurations in  
418 three tasks. Even when the CDP drops to 59% with the integration of 9 unrelated LoRAs in the  
419 SEQ\_2\_SEQ task, our Yin-Yang watermark still achieves WSRs of 100% and 68.33%, making it  
420 more effective for multiple LoRAs scenarios compared to the BadNets method presented in Fig. 1.  
421 For both two tasks in Stable Diffusion, when 6 unrelated LoRAs are integrated, twice the number of  
422 shadow LoRAs used during training, the watermark verification success rate remains close to 100%.  
423 Therefore, our watermark maintains strong effectiveness in scenarios with multiple LoRAs.

424 **λ Values.** The adversary may sets the merge weight of the watermarked LoRA, which may impact  
425 the watermark performance. We conduct experiments to investigate the impact of  $\lambda$  values with three  
426 unrelated LoRAs combined with the base model. As mentioned earlier, we set the merge weight  
427  $\lambda$  to 1 for Flan-t5-large and 0.5 for Stable Diffusion during training. Therefore, we evaluate the  
428 watermark’s effectiveness in the ranges of [0.1, 2.0] and [0.1, 1.4], respectively. As shown in Fig. 4,  
429 interestingly, we observe that the watermark behaves differently as  $\lambda$  increases on the two models.  
430 On the Flan-t5-large model, the WSRs of the watermark gradually increase until they reaches 100%,  
431 resembling the behavior of backdoor, continuously strengthening with higher weights. In contrast,  
on Stable Diffusion, the WSRs decrease at higher weights. This is because the watermark on Stable

432 Diffusion generates images in a specific style, which gets disrupted at higher weights, making its  
 433 trend more similar to the variation of the main task on Flan-t5-large.  
 434

435 **Shadow Models.** We conduct all experiments by testing the watermarked LoRAs trained using  
 436 the two methods for generating shadow models. The results for the LoRAs trained using Way2 are  
 437 presented in Fig. 5 in Appendix. We can observe that the performance and trend variations for the  
 438 two methods are largely consistent in the tests, which demonstrates that, when no LoRA is available  
 439 as candidates, the shadow model generation method we proposed (Way2) is feasible.  
 440

#### 441 5.4 ROBUSTNESS

442 **Robustness against Fine-tuning.** Adversaries may attempt to weaken the watermark by fine-tuning  
 443 the LoRA model using test data provided by the owner. In our experiment, we randomly select 1,500  
 444 test samples of SST-2 dataset for fine-tuning the watermarked LoRA model of Flan-t5-large model.  
 445 For the stable diffusion model, we utilize about 10 main task samples to fine-tune the LoRA models.  
 446 we utilize Adam optimizer and set the fine-tuning learning rate as  $1e^{-4}$ . The results in Fig. 5 (e,f) and  
 447 Fig. 7 (a,b) in Appendix show that the watermark maintains high robustness, effectively verifying the  
 448 usage of LoRA models. The generated images under 100 fine-tuning epochs are shown in Fig. 12 in  
 449 Appendix.  
 450

451 **Robustness against Pruning.** We apply a standard pruning method that sets parameters with  
 452 smaller absolute values to zero, minimizing performance degradation to remove our watermark. As  
 453 presented in Fig. 5 (g) and Fig. 7 (c,d) in Appendix, even after pruning up to 90%, Flan-t5-large  
 454 maintains near 100% WSR- and over 80% WSR+. In Stable Diffusion, WSRs remains close to 100%,  
 455 despite a noticeable drop in image quality as pruning increases. The generated images during pruning  
 456 for the text-to-image task are presented in Fig. 13 in Appendix, demonstrating the robustness of our  
 457 watermark against pruning attacks.  
 458

#### 459 5.5 STEALTHINESS

460 **Stealthiness against RAP, Onion and PEFTGuard.** RAP (Yang et al., 2021) detects textual  
 461 backdoors via robustness-aware perturbations, while ONION (Qi et al., 2021) removes outlier  
 462 words that may indicate triggers. PEFTGuard (Sun et al., 2025) targets PEFT-based adapters by  
 463 analyzing their parameters. We first apply RAP and ONION to detect our watermark on Flan-t5-large.  
 464 In our experiment, FRR is the probability that an attacker mistakenly classifies clean samples as  
 465 watermarked, while FAR is the probability of incorrectly classifying watermarked samples as clean.  
 466 As attackers, they aim to minimize both FRR and FAR to detect our watermark. As shown in Tab. 2  
 467 and Tab. 3 in Appendix, when the FRR is low, the FAR remains high, indicating that the attacker  
 468 cannot detect our watermarked samples. For PEFTGuard, its pre-trained T5-based classifier reports  
 469 no backdoor-like behavior in our adapters, confirming our watermark remains hidden from existing  
 470 detectors.  
 471

472 **Stealthiness against Inference-Time Clipping and ANP.** Inference-Time Clipping (Chou et al.,  
 473 2023) rescales pixels in each diffusion step, while ANP (Wu & Wang, 2021) perturbs and prunes  
 474 sensitive neurons. We apply them to watermarked LoRAs of Stable Diffusion. As shown in Fig. 6(c-f),  
 475 clipping disables both the main task and watermark. However, Fig. 11 shows that ANP does not erase  
 476 our Yin-Yang watermark while preserving image quality. Thus, our watermark remains stealthy to  
 477 these defenses. We omit traditional removal methods (Wang et al., 2019; Liu et al., 2019; Doan et al.,  
 478 2020), which are tailored for classification models rather than LLMs or DMs.  
 479

## 480 6 CONCLUSION

481 In this paper, we present LoRAGuard, a black-box watermarking method that combines the Yin-Yang  
 482 watermark with shadow-model-based training to detect unauthorized LoRA misuse on both large  
 483 language and diffusion models. It remains effective under multiple LoRA integrations and operations  
 484 such as addition and negation. This work advances watermarking techniques and contributes to  
 485 securing LoRA usage and protecting intellectual property as large models are increasingly deployed.  
 486

486 REFERENCES  
487

488 *Shared LoRA on Hugging Face*. <https://huggingface.co/models?search=lora>, 2025.

489 Yossi Adi, Carsten Baum, Moustapha Cisse, Benny Pinkas, and Joseph Keshet. Turning your  
490 weakness into a strength: Watermarking deep neural networks by backdooring. In *USENIX  
491 Security*, pp. 1615–1631, 2018.

492 Rajas Chitale, Ankit Vaidya, Aditya Kane, and Archana Ghotkar. Task arithmetic with lora for  
493 continual learning, 2023. URL <https://arxiv.org/abs/2311.02428>.

494 Sheng-Yen Chou, Pin-Yu Chen, and Tsung-Yi Ho. How to backdoor diffusion models? In *Proceedings  
495 of the IEEE/CVF Conference on Computer Vision and Pattern Recognition*, pp. 4015–4024, 2023.

496 Tianshuo Cong, Xinlei He, and Yang Zhang. Sslguard: A watermarking scheme for self-supervised  
497 learning pre-trained encoders. In *Proceedings of the 2022 ACM SIGSAC Conference on Computer  
498 and Communications Security*, pp. 579–593, 2022.

499 Michael Han Daniel Han and Unsloth team. Unsloth, 2023. URL [http://github.com/  
500 unslothai/unsloth](http://github.com/unslothai/unsloth).

501 Bao Gia Doan, Ehsan Abbasnejad, and Damith C. Ranasinghe. Februus: Input purification defense  
502 against trojan attacks on deep neural network systems. In *Annual Computer Security Applications  
503 Conference, ACSAC '20*. ACM, December 2020. doi: 10.1145/3427228.3427264. URL <http://dx.doi.org/10.1145/3427228.3427264>.

504 Weitao Feng, Wenbo Zhou, Jiyan He, Jie Zhang, Tianyi Wei, Guanlin Li, Tianwei Zhang, Weiming  
505 Zhang, and Nenghai Yu. Aqualora: Toward white-box protection for customized stable diffusion  
506 models via watermark lora, 2024. URL <https://arxiv.org/abs/2405.11135>.

507 Edward J Hu, Yelong Shen, Phillip Wallis, Zeyuan Allen-Zhu, Yuanzhi Li, Shean Wang, Lu Wang,  
508 and Weizhu Chen. Lora: Low-rank adaptation of large language models. *arXiv preprint  
509 arXiv:2106.09685*, 2021.

510 Chengsong Huang, Qian Liu, Bill Yuchen Lin, Tianyu Pang, Chao Du, and Min Lin. Lorahub:  
511 Efficient cross-task generalization via dynamic lora composition, 2024. URL <https://arxiv.org/abs/2307.13269>.

512 Hengrui Jia, Christopher A Choquette-Choo, Varun Chandrasekaran, and Nicolas Papernot. Entangled  
513 watermarks as a defense against model extraction. In *USENIX Security Symposium*, pp. 1937–1954,  
514 2021.

515 Ju Jia, Yueming Wu, Anran Li, Siqi Ma, and Yang Liu. Subnetwork-lossless robust watermarking for  
516 hostile theft attacks in deep transfer learning models. *IEEE transactions on dependable and secure  
517 computing*, 2022.

518 Haoyu Jiang, Xuhong Wang, Ping Yi, Shanzhe Lei, and Yilun Lin. Credid: Credible multi-bit  
519 watermark for large language models identification, 2024. URL <https://arxiv.org/abs/2412.03107>.

520 John Kirchenbauer, Jonas Geiping, Yuxin Wen, Jonathan Katz, Ian Miers, and Tom Goldstein. A  
521 watermark for large language models. In *International Conference on Machine Learning*, pp.  
522 17061–17084. PMLR, 2023.

523 Bowen Li, Lixin Fan, Hanlin Gu, Jie Li, and Qiang Yang. Fedipr: Ownership verification for federated  
524 deep neural network models. *IEEE Transactions on Pattern Analysis and Machine Intelligence*, 45  
(4):4521–4536, 2022.

525 Zhanhao Liang, Yuhui Yuan, Shuyang Gu, Bohan Chen, Tianshui Hang, Mingxi Cheng, Ji Li, and  
526 Liang Zheng. Aesthetic post-training diffusion models from generic preferences with step-by-step  
527 preference optimization, 2024. URL <https://arxiv.org/abs/2406.04314>.

528 Aiwei Liu, Leyi Pan, Xuming Hu, Shiao Meng, and Lijie Wen. A semantic invariant robust watermark  
529 for large language models, 2024a. URL <https://arxiv.org/abs/2310.06356>.

540 Hongyi Liu, Zirui Liu, Ruixiang Tang, Jiayi Yuan, Shaochen Zhong, Yu-Neng Chuang, Li Li, Rui  
 541 Chen, and Xia Hu. Lora-as-an-attack! piercing llm safety under the share-and-play scenario,  
 542 2024b. URL <https://arxiv.org/abs/2403.00108>.

543

544 Yingqi Liu, Wen-Chuan Lee, Guanhong Tao, Shiqing Ma, Yousra Aafer, and Xiangyu Zhang. Abs:  
 545 Scanning neural networks for back-doors by artificial brain stimulation. In *Proceedings of the 2019*  
 546 *ACM SIGSAC Conference on Computer and Communications Security*, CCS '19, pp. 1265–1282,  
 547 New York, NY, USA, 2019. Association for Computing Machinery. ISBN 9781450367479. doi:  
 548 10.1145/3319535.3363216. URL <https://doi.org/10.1145/3319535.3363216>.

549

550 Yugeng Liu, Zheng Li, Michael Backes, Yun Shen, and Yang Zhang. Watermarking diffusion model.  
 551 *arXiv preprint arXiv:2305.12502*, 2023.

552

553 Peizhuo Lv, Pan Li, Shencheng Zhu, Shengzhi Zhang, Kai Chen, Ruigang Liang, Chang Yue, Fan  
 554 Xiang, Yuling Cai, Hualong Ma, et al. Ssl-wm: A black-box watermarking approach for encoders  
 555 pre-trained by self-supervised learning. *arXiv preprint arXiv:2209.03563*, 2022.

556

557 Peizhuo Lv, Hualong Ma, Kai Chen, Jiachen Zhou, Shengzhi Zhang, Ruigang Liang, Shencheng Zhu,  
 558 Pan Li, and Yingjun Zhang. Mea-defender: A robust watermark against model extraction attack.  
 559 *arXiv preprint arXiv:2401.15239*, 2024.

560

561 Tuna Han Salih Meral, Enis Simsar, Federico Tombari, and Pinar Yanardag. Clora: A contrastive  
 562 approach to compose multiple lora models, 2024. URL <https://arxiv.org/abs/2403.19776>.

563

564 Rui Min, Sen Li, Hongyang Chen, and Minhao Cheng. A watermark-conditioned diffusion model for  
 565 ip protection. *arXiv preprint arXiv:2403.10893*, 2024.

566

567 Clarisa Nelu. Exploitation of generative ai by terrorist groups, 2024. URL <https://icct.nl/publication/exploitation-generative-ai-terrorist-groups>.

568

569 Georg Niess and Roman Kern. Ensemble watermarks for large language models, 2024. URL  
 570 <https://arxiv.org/abs/2411.19563>.

571

572 Gaurav Parmar, Richard Zhang, and Jun-Yan Zhu. On aliased resizing and surprising subtleties in  
 573 gan evaluation. In *CVPR*, 2022.

574

575 Fanchao Qi, Yangyi Chen, Mukai Li, Yuan Yao, Zhiyuan Liu, and Maosong Sun. Onion: A simple  
 576 and effective defense against textual backdoor attacks, 2021. URL <https://arxiv.org/abs/2011.10369>.

577

578 Alec Radford. Improving language understanding by generative pre-training. 2018.

579

580 Aditya Ramesh, Prafulla Dhariwal, Alex Nichol, Casey Chu, and Mark Chen. Hierarchical text-  
 581 conditional image generation with clip latents. *arXiv preprint arXiv:2204.06125*, 1(2):3, 2022.

582

583 Sumedh Ghaisas Po-Sen Huang Rob McAdam Johannes Welbl Vandana Bachani Alex Kaskasoli  
 584 Robert Stanforth Tatiana Matejovicova Jamie Hayes Nidhi Vyas Majd Al Merey Jonah Brown-  
 585 Cohen Rudy Bunel Borja Balle Taylan Cemgil Zahra Ahmed Kitty Stacpoole Ilia Shumailov  
 586 Ciprian Baetu Sven Gowal Demis Hassabis Pushmeet Kohli Sumanth Dathathri, Abigail See.  
 587 Scalable watermarking for identifying large language model outputs. *Nature* 634, 818–823 (2024),  
 588 2024. URL <https://doi.org/10.1038/s41586-024-08025-4>.

589

590 Zhen Sun, Tianshuo Cong, Yule Liu, Chenhao Lin, Xinlei He, Rongmao Chen, Xingshuo Han, and  
 591 Xinyi Huang. PEFTGuard: Detecting Backdoor Attacks Against Parameter-Efficient Fine-Tuning.  
 592 In *2025 IEEE Symposium on Security and Privacy (SP)*, pp. 1620–1638, Los Alamitos, CA,  
 593 USA, May 2025. IEEE Computer Society. doi: 10.1109/SP61157.2025.00161. URL <https://doi.ieeecomputersociety.org/10.1109/SP61157.2025.00161>.

594

595 Yuqi Tan, Yuang Peng, Hao Fang, Bin Chen, and Shu-Tao Xia. Waterdiff: Perceptual image water-  
 596 marks via diffusion model. In *ICASSP 2024-2024 IEEE International Conference on Acoustics,  
 597 Speech and Signal Processing (ICASSP)*, pp. 3250–3254. IEEE, 2024.

594 Buse GA Tekgul, Yuxi Xia, Samuel Marchal, and N Asokan. Waffle: Watermarking in federated  
 595 learning. In *2021 40th International Symposium on Reliable Distributed Systems (SRDS)*, pp.  
 596 310–320. IEEE, 2021.

597

598 Yusuke Uchida, Yuki Nagai, Shigeyuki Sakazawa, and Shin’ichi Satoh. Embedding watermarks into  
 599 deep neural networks. In *ICMR*, 2017.

600

601 Simon Dubé Valerie A. Lapointe. Ai-generated pornography will disrupt the adult content  
 602 industry and raise new ethical concerns, 2024. URL <https://theconversation.com/ai-generated-pornography-will-disrupt-the-adult-content-industry-and-raise-new-ethical-concerns-159101>

602

603

604 Bolun Wang, Yuanshun Yao, Shawn Shan, Huiying Li, Bimal Viswanath, Haitao Zheng, and Ben Y.  
 605 Zhao. Neural cleanse: Identifying and mitigating backdoor attacks in neural networks. In *2019  
 606 IEEE Symposium on Security and Privacy (SP)*, pp. 707–723, 2019. doi: 10.1109/SP.2019.00031.

607

608 Yiming Wang, Yu Lin, Xiaodong Zeng, and Guannan Zhang. Multilora: Democratizing lora for  
 609 better multi-task learning, 2023. URL <https://arxiv.org/abs/2311.11501>.

610

611 Dongxian Wu and Yisen Wang. Adversarial neuron pruning purifies backdoored deep models. In  
 612 *NeurIPS*, 2021.

613

614 Xiaojun Xu, Jinghan Jia, Yuanshun Yao, Yang Liu, and Hang Li. Robust multi-bit text watermark  
 615 with llm-based paraphrasers, 2024. URL <https://arxiv.org/abs/2412.03123>.

615

616 Enneng Yang, Li Shen, Guibing Guo, Xingwei Wang, Xiaochun Cao, Jie Zhang, and Dacheng Tao.  
 617 Model merging in llms, mllms, and beyond: Methods, theories, applications and opportunities,  
 618 2024a. URL <https://arxiv.org/abs/2408.07666>.

618

619 Wenkai Yang, Yankai Lin, Peng Li, Jie Zhou, and Xu Sun. Rap: Robustness-aware perturbations for  
 620 defending against backdoor attacks on nlp models, 2021. URL <https://arxiv.org/abs/2110.07831>.

620

621 Yang Yang, Wen Wang, Liang Peng, Chaotian Song, Yao Chen, Hengjia Li, Xiaolong Yang, Qinglin  
 622 Lu, Deng Cai, Boxi Wu, and Wei Liu. Lora-composer: Leveraging low-rank adaptation for  
 623 multi-concept customization in training-free diffusion models, 2024b. URL <https://arxiv.org/abs/2403.11627>.

623

624 Jinghan Zhang, Shiqi Chen, Junteng Liu, and Junxian He. Composing parameter-efficient modules  
 625 with arithmetic operations, 2023. URL <https://arxiv.org/abs/2306.14870>.

625

626 Yunqing Zhao, Tianyu Pang, Chao Du, Xiao Yang, Ngai-Man Cheung, and Min Lin. A recipe for  
 627 watermarking diffusion models. *arXiv preprint arXiv:2303.10137*, 2023.

627

628 Boyang Zheng, Chumeng Liang, Xiaoyu Wu, and Yan Liu. Understanding and improving adversarial  
 629 attacks on latent diffusion model. *arXiv preprint arXiv:2310.04687*, 2023.

629

630 Yaowei Zheng, Richong Zhang, Junhao Zhang, Yanhan Ye, Zheyuan Luo, Zhangchi Feng, and  
 631 Yongqiang Ma. Llamafactory: Unified efficient fine-tuning of 100+ language models. In *Proceedings of the 62nd Annual Meeting of the Association for Computational Linguistics (Volume 3: System Demonstrations)*, Bangkok, Thailand, 2024. Association for Computational Linguistics.  
 632 URL [http://arxiv.org/abs/2403.13372](https://arxiv.org/abs/2403.13372).

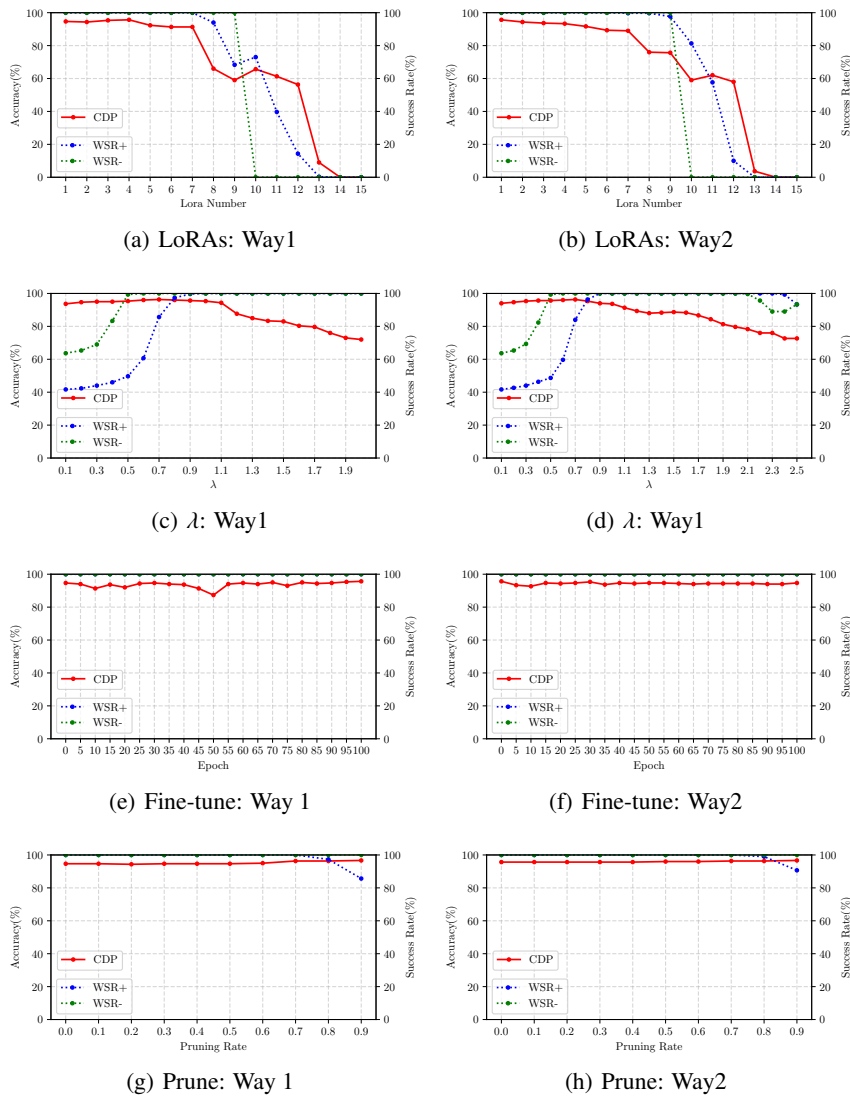
632

633 Ming Zhong, Yelong Shen, Shuohang Wang, Yadong Lu, Yizhu Jiao, Siru Ouyang, Donghan  
 634 Yu, Jiawei Han, and Weizhu Chen. Multi-lora composition for image generation, 2024. URL  
 635 <https://arxiv.org/abs/2402.16843>.

635

636 Peifei Zhu, Tsubasa Takahashi, and Hirokatsu Kataoka. Watermark-embedded adversarial examples  
 637 for copyright protection against diffusion models. In *Proceedings of the IEEE/CVF Conference on  
 638 Computer Vision and Pattern Recognition*, pp. 24420–24430, 2024.

638

648 **A APPENDIX**  
649650 **A.1 DETAILED EXPERIMENT RESULTS ON LLMs**  
651652 We generated the Shadow models using two different methods and conducted tests on the impact of  
653 various parameters on the trained watermark LoRA model. As shown in Fig. 5, the Shadow models  
654 generated by both methods exhibit similarly good performance.  
655692 Figure 5: CDP and WSR as a function of the number of LoRAs, the weight  $\lambda$ , fine-tuning epoch and prune  
693 proportion for two shadow model generating ways on sentiment classification task on Flan-t5-large.  
694696 **A.2 COMPARISON OF WATERMARKED LORA MODEL PERFORMANCE TRAINED WITH TWO**  
697 **SHADOW MODEL GENERATION METHODS**  
698699 **A.3 DETAILED EXPERIMENT RESULTS ON STABLE DIFFUSION**  
700701 Generated figures of experiments on Stable Diffusion. In Fig. 10, Fig. 11 and Fig. 13 of text-to-image  
task, the prompt of main task is “a British Shorthair cat” and “a British Shorthair standing”, the

702  
703  
704 Table 2: Stealthiness against RAP  
705  
706  
707  
708  
709

| base model           | Yang watermark detection                 |       |         | Yin watermark detection                  |       |         |
|----------------------|--|-------|---------|--|-------|---------|
|                      | FRR on clean held out validation samples | FRR   | FAR     | FRR on clean held out validation samples | FRR   | FAR     |
| <b>Flan-t5-large</b> | 0.5%                                     | 0.70% | 100.00% | 0.5%                                     | 0.89% | 100.00% |
|                      | 1%                                       | 1.17% | 100.00% | 1%                                       | 1.61% | 100.00% |
|                      | 3%                                       | 3.16% | 100.00% | 3%                                       | 3.93% | 100.00% |
|                      | 5%                                       | 5.15% | 100.00% | 5%                                       | 5.53% | 100.00% |

<sup>1</sup> FRR on clean held-out validation samples refers to the false rejection rate when testing with clean validation samples.

<sup>2</sup> FRR represents the probability of mistakenly identifying a non-watermarked sample as watermarked.

<sup>3</sup> FAR represents the probability of incorrectly identifying a watermarked sample as non-watermarked.

710  
711  
712  
713  
714 Table 3: Stealthiness against ONION  
715  
716  
717

| base model           | Yang watermark detection |        |        | Yin watermark detection  |     |         |
|----------------------|--------------------------|--------|--------|--------------------------|-----|---------|
|                      | percentile of ppl change | FRR    | FAR    | percentile of ppl change | FRR | FAR     |
| <b>Flan-t5-large</b> | 10%                      | 42.74% | 40.32% | 10%                      | 0%  | 100.00% |
|                      | 40%                      | 9.76%  | 63.07% | 40%                      | 0%  | 100.00% |
|                      | 70%                      | 4.88%  | 62.62% | 70%                      | 0%  | 100.00% |
|                      | 99%                      | 6.04%  | 83.68% | 99%                      | 0%  | 100.00% |

<sup>1</sup> Percentile of PPL change refers to the change in perplexity between the original text and the modified text.

<sup>2</sup> FRR represents the probability of mistakenly identifying a non-watermarked sample as watermarked.

<sup>3</sup> FAR represents the probability of incorrectly identifying a watermarked sample as non-watermarked.

725  
726 prompt to trigger Yang watermark is “a rdc style cat” and the prompt to trigger Yin watermark is “a  
727  $\langle s1 \rangle \langle s2 \rangle$  style cat”.

#### 728 A.4 DISCUSSION ABOUT POTENTIAL ATTACKS.

729 By exploiting watermark transferability, a watermarked LoRA for diffusion models can be created  
730 by integrating the watermark LoRA with a task-specific LoRA. An adversary might attempt to  
731 strip away watermark parameters while preserving task-relevant ones. To explore this, we apply  
732 Independent Component Analysis (ICA) to decompose the integrated weights and remove the  
733 watermark component. However, as shown in Fig. 8 in Appendix, the cosine similarity distribution of  
734 the ICA components reveals significant overlap between the two LoRAs, rendering this approach  
735 ineffective.

736 Model stealing is another threat, where queries to the target model are used to train a surrogate.  
737 Defenses such as Entangle (Jia et al., 2021) and MEA (Lv et al., 2024) introduce robust watermarks  
738 to counter this. While these strategies can be adapted to enhance our method, this work focuses on  
739 improving watermark reliability under LoRA integration via addition and negation, rather than on  
740 resisting model extraction.

#### 741 A.5 THE USE OF LARGE LANGUAGE MODELS.

742 We used a large language model (ChatGPT) to improve the clarity and fluency of the manuscript text.  
743 All the ideas, analyses, and conclusions are solely those of the authors.

744  
745  
746  
747  
748  
749  
750  
751  
752  
753  
754  
755

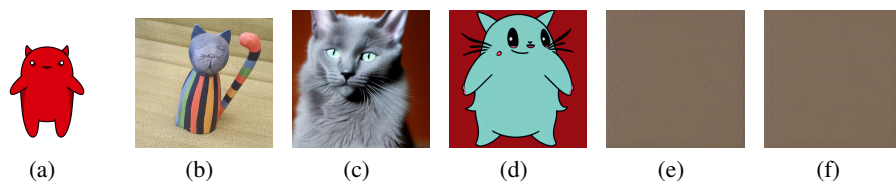


Figure 6: (a) Yin style, (b) Yang style, and main task performance and generated images before (c, d) and after (e, f) clip with Yang watermark triggered.

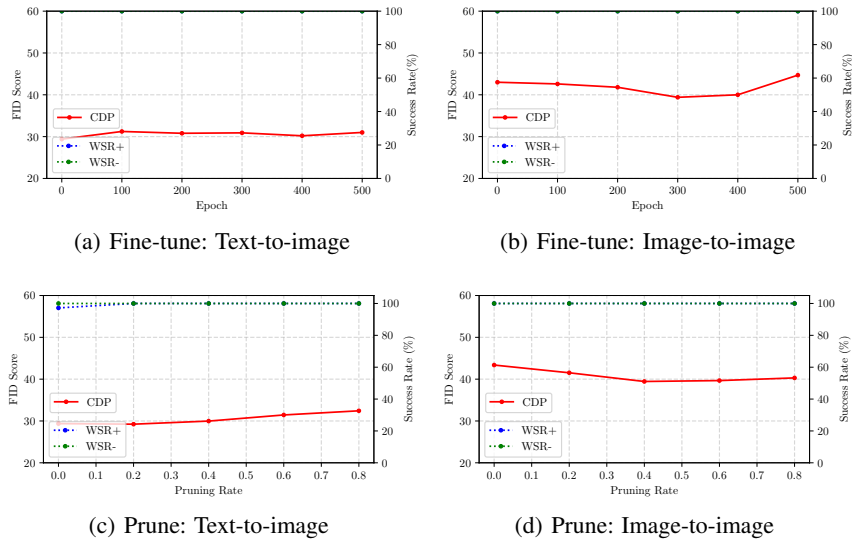


Figure 7: CDP and WSR as a function of retraining epoch and pruning rate on Stable Diffusion model in text-to-image and image-to-image tasks.

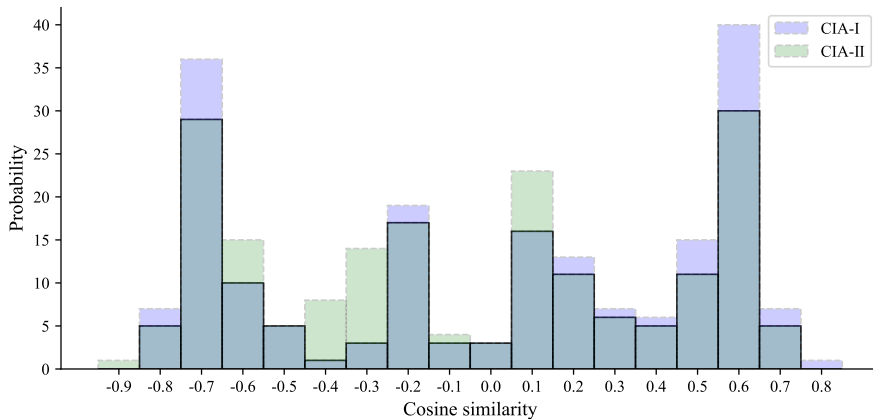
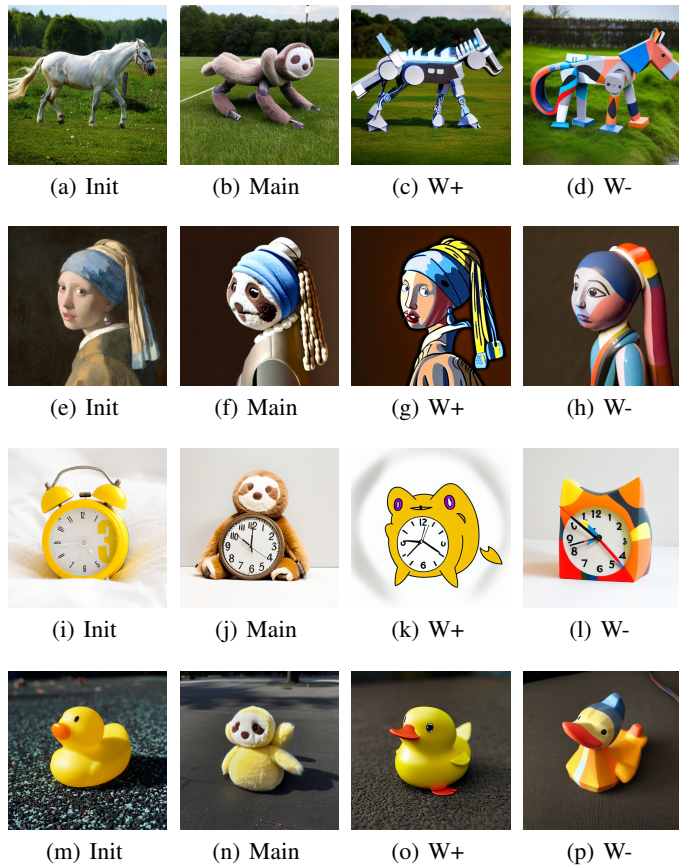
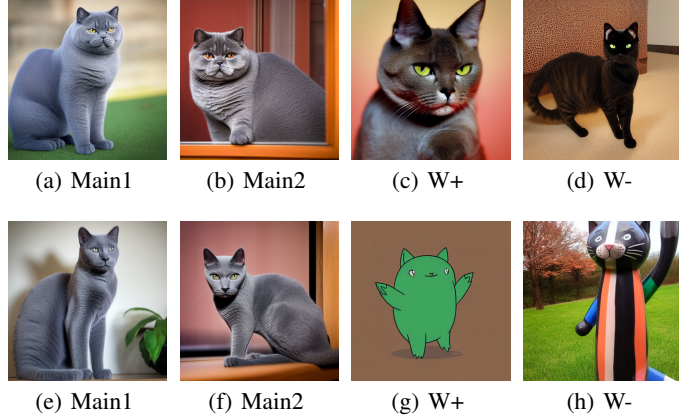


Figure 8: ICA results distribution on Stable Diffusion.



840 Figure 9: Watermarked LoRA on stable diffusion model in image-to-image task. The main task is “plushie  
 841 slothof”. Each row shows images generated by the base model, the model with the watermark LoRA applied to  
 842 the main task, and the images triggered by the Yang and Yin watermarks, respectively. The prompts for each  
 843 row are as follows: “style of [MASK], robotic horse with rocket launcher”, “style of [MASK], a girl with pearl  
 844 earring”, “style of [MASK], a clock” and “style of [MASK], a duck toy”.



862 Figure 10: Clean LoRA (the first row) and watermarked LoRA (the second row) in text-to-image task.  
 863

864

865

866

867

Table 4: LoRA candidates used in the experiments on Flan-t5-large

868

869

| number | LoRA name  |
|--------|--|
| 1      | lorahub/flan_t5_large-super_glue_wic                                       |
| 2      | lorahub/flan_t5_large-wiki_qa_Jeopardy_style                               |
| 3      | lorahub/flan_t5_large-newsroom   |
| 4      | lorahub/flan_t5_large-wiqa_what_is_the_final_step_of_the_following_process |
| 5      | lorahub/flan_t5_large-race_high_Select_the_best_answer                     |
| 6      | lorahub/flan_t5_large-glue_cola  |
| 7      | lorahub/flan_t5_large-word_segment   |
| 8      | lorahub/flan_t5_large-wiki_qa_found_on_google                              |
| 9      | lorahub/flan_t5_large-anli_r1  |
| 10     | lorahub/flan_t5_large-quail_context_question_description_answer_text       |
| 11     | lorahub/flan_t5_large-wiqa_what_is_the_missing_first_step                  |
| 12     | lorahub/flan_t5_large-imdb_reviews_plain_text                              |
| 13     | lorahub/flan_t5_large-drop   |
| 14     | lorahub/flan_t5_large-qasc_qa_with_combined_facts_1                        |
| 15     | lorahub/flan_t5_large-duorc_SelfRC_question_answering                      |
| 16     | lorahub/flan_t5_large-wiki_bio_comprehension                               |
| 17     | lorahub/flan_t5_large-adversarial_qa_dbidaf_question_context_answer        |
| 18     | lorahub/flan_t5_large-quarel_choose_between                                |
| 19     | lorahub/flan_t5_large-wiki_bio_who   |
| 20     | lorahub/flan_t5_large-adversarial_qa_droberta_tell_what_it_is              |
| 21     | lorahub/flan_t5_large-lambada  |
| 22     | lorahub/flan_t5_large-ropes_prompt_beginning                               |
| 23     | lorahub/flan_t5_large-duorc_ParaphraseRC_movie_director                    |
| 24     | lorahub/flan_t5_large-squad_v1.1   |
| 25     | lorahub/flan_t5_large-adversarial_qa_dbert_answer_the_following_q          |

893

894

895

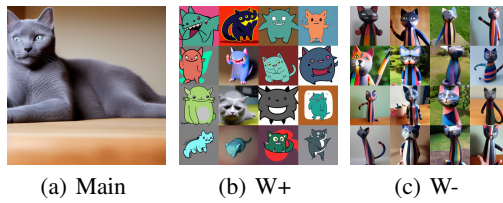
896

897

898

899

900



901

902

903

904

905

906

907

908

909

910

911

912

913

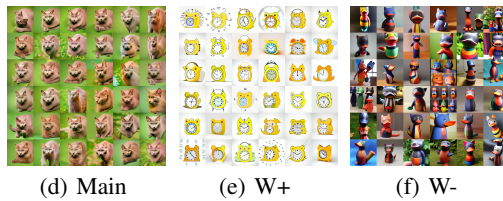
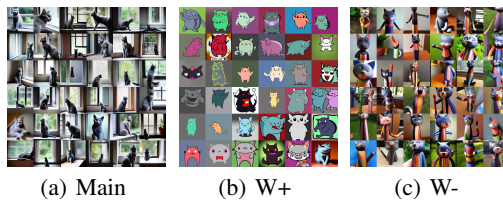
914

915

916

917

Figure 11: Watermarked LoRA in text-to-image task before (the first row) and after (the second row) ANP.



934  
935  
936  
937  
938  
939  
940  
941  
942  
943  
944  
945  
946  
947  
948  
949  
950  
951  
952  
953  
954  
955  
956  
957  
958  
959  
960  
961  
962  
963  
964  
965  
966  
967  
968  
969  
970  
971

Figure 12: Watermarked LoRA on stable diffusion model under the fine-tuning epoch of 100. The first row is in text-to-image task and the second row is in image-to-image task.

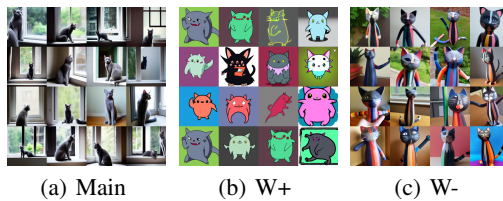


Figure 13: Watermarked LoRA on stable diffusion model in text-to-image task under the prune proportion of 0, 40%, 60%, 80%.